Microfireball Propagation in Z-Discharge Plasma Channels in the Light Ion Fusion Target Development Facility

Robert R. Peterson, John J. Watrous and Gregory A. Moses

January 1985

UWFDM-613

FUSION TECHNOLOGY INSTITUTE

UNIVERSITY OF WISCONSIN

MADISON WISCONSIN

Microfireball Propagation in Z-Discharge Plasma Channels in the Light Ion Fusion Target Development Facility

Robert R. Peterson, John J. Watrous and Gregory A. Moses

Fusion Technology Institute
University of Wisconsin
1500 Engineering Drive
Madison, WI 53706

http://fti.neep.wisc.edu

January 1985

UWFDM-613

MICROFIREBALL PROPAGATION IN Z-DISCHARGE PLASMA CHANNELS IN THE LIGHT ION FUSION TARGET DEVELOPMENT FACILITY

Robert R. Peterson

John J. Watrous

Gregory A. Moses

Fusion Technology Institute
1500 Johnson Drive
University of Wisconsin-Madison
Madison, Wisconsin 53706

January 1985

UWFDM-613

1. Introduction

Laser initiated z-discharge plasma channels are a promising approach for transporting beams of 1 to 100 MeV light ions from ion diodes to an inertial confinement fusion target.[1-3] These channels could be formed by creating paths of ionization with a system of lasers. These preionized paths would then carry an electrical discharge.[4-8] The electron current making up the discharge would rarify the channels and create an azimuthal magnetic field. At the proper time during the pinch of the channel, the ion beam would be injected into the channel and these ions would be confined to the channel by the azimuthal magnetic fields provided by the channel current. A potential problem with this system is that the plasma channels are still present at the time of target ignition and burn, and they may "channel" the energy of the target generated microfireball into the diodes. It is the purpose of the work presented here to study the propagation of these microfireballs in the z-discharge plasma channels.

The Light Ion Fusion Target Development Facility (TDF) would be the first system in which light ion beams are focused onto reactor sized targets at a rate of at least ten times a day, imploding them to ignition.[9] Representative parameters for the TDF are given in Table 1. Ion transport in z-discharge plasma channels is proposed for the TDF to provide a stand-off distance that protects the diodes. A schematic picture of the TDF is shown in Fig. 1.

There are three general classes of phenomena occurring in a plasma channel: (1) channel formation and beam transmission, (2) radial expansion of the channel with reduction of the on-axis density, and (3) dissipation of the channel and return to uniform conditions in the gas. These take place over

Table 1. Light Ion Fusion Target Development Facility Parameters

Nominal Target Yield (MJ)	200
Distance from Target to First Wall of Target Chamber (m)	3
Length of Channels (m)	4
Diameter of Channels (cm)	1
Target Chamber Gas Species	Molecular Nitrogen
Initial Temperature of Channel Center (eV)	35
Initial Background of Channel Center (eV)	0.025
Initial Density of Channel Center (g/cm^3)	9.9×10^{-6}
Initial Background Gas Density (g/cm^3)	2.25×10^{-5}

LIGHT ION FUSION TARGET DEVELOPMENT FACILITY

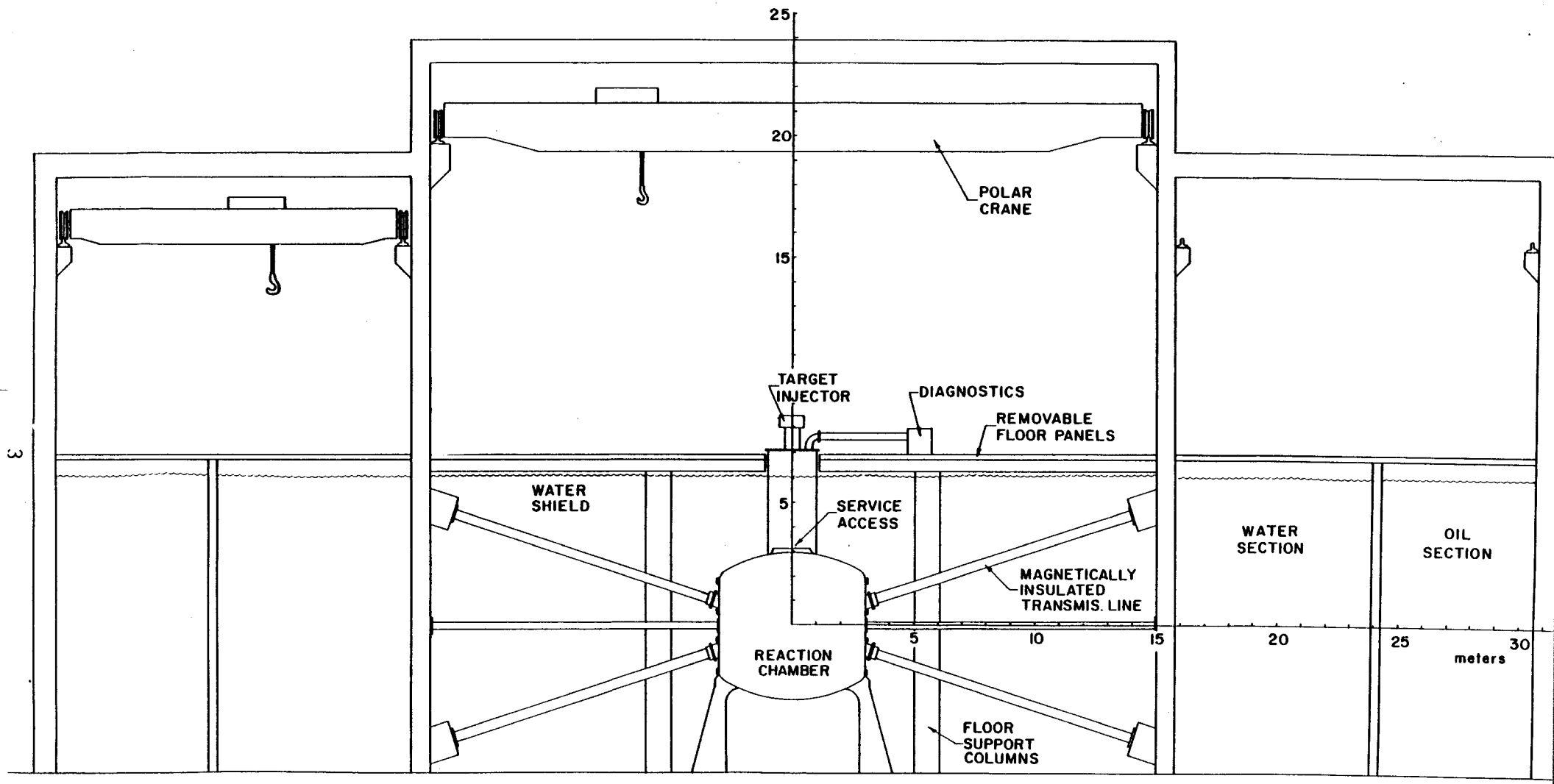

Fig. 1. Schematic Picture of the Light Ion Fusion Target Development Facility.

different time periods as shown in the timeline in Fig. 2. Also shown on the timeline is the propagation of the microfireball. The channel formation and beam transmission phase is very early, ending in a few microseconds, so it is independent of the propagation of the microfireball. After the ion beam has completed its passage down the channel, the now very hot channel rapidly expands and transports energy radially out into the cold background gas. At roughly the same time the microfireball has begun its trip down the plasma channel so these two phenomena can affect each other. After a few hundred microseconds the microfireball has reached the end of the channel, the outward radial motion of the channel has ceased, and the gas begins to return to uniformity.

The microfireball propagation is truly a two- or three-dimensional process when it occurs in the presence of plasma channels. A schematic picture of the channel and microfireball system is shown in Fig. 3. The microfireball will show both energy and momentum transport along the axis of each channel. The energy of the microfireball will also move radially out from the channel into the cold background gas and the high temperature of the microfireball will cause a large radial pressure gradient that drives the channel radially outward. In the event that the radial expansion of the channels pushes them into each other, the behavior of the microfireball propagation is three-dimensional. We have attempted to model the two-dimensional behavior with the use of two one-dimensional radiation-hydrodynamic computer simulation codes in series. Previously a numerical simulation of this phenomenon was attempted, where the expansion of the channel due to the microfireball was neglected and a one group diffusion model was used for the radiative heat transfer.[10] In this paper, we will present computer simulations resulting from the use of an

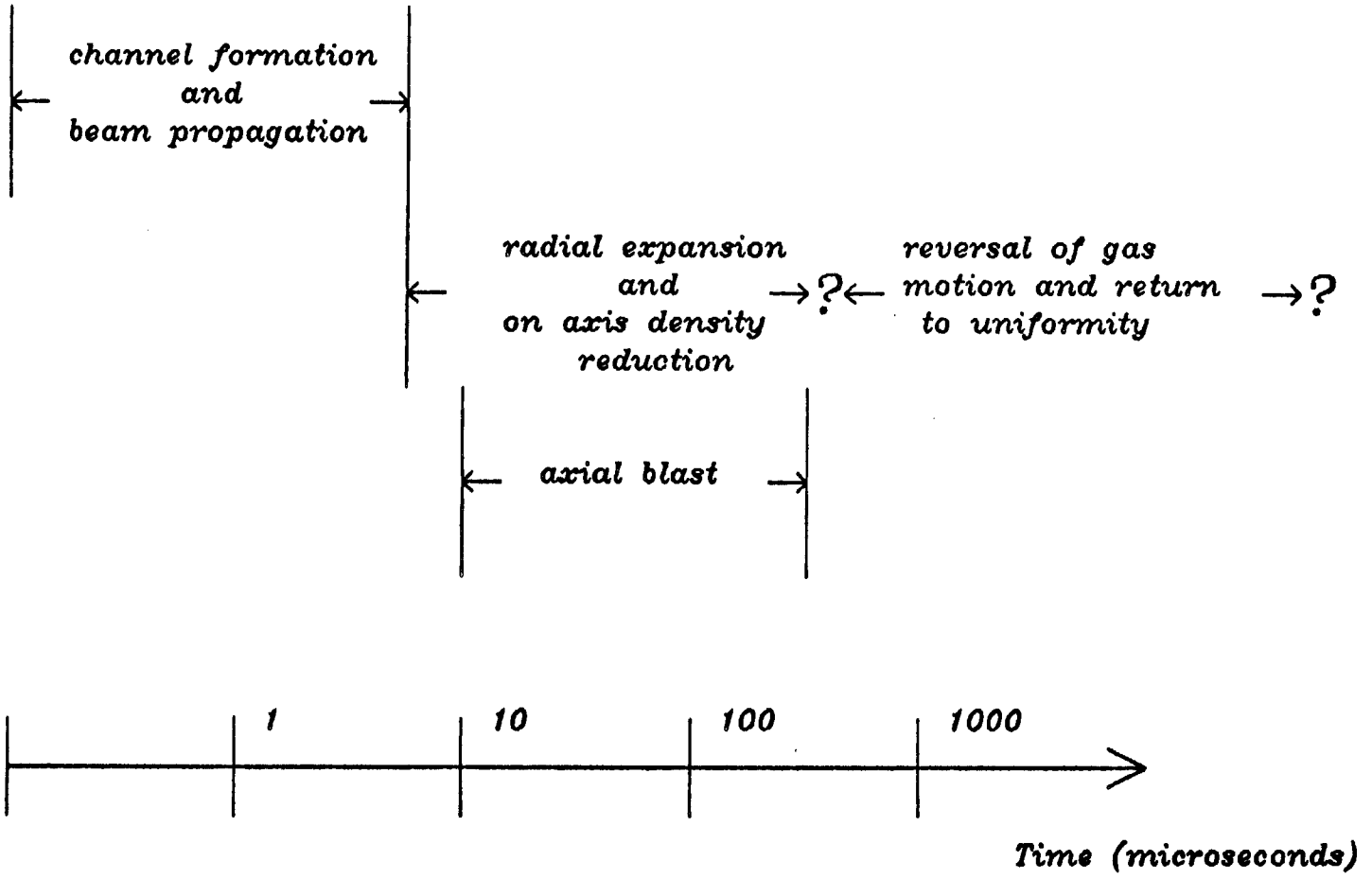

Fig. 2 Timeline for Microfireball in Plasma Channel Phenomena.

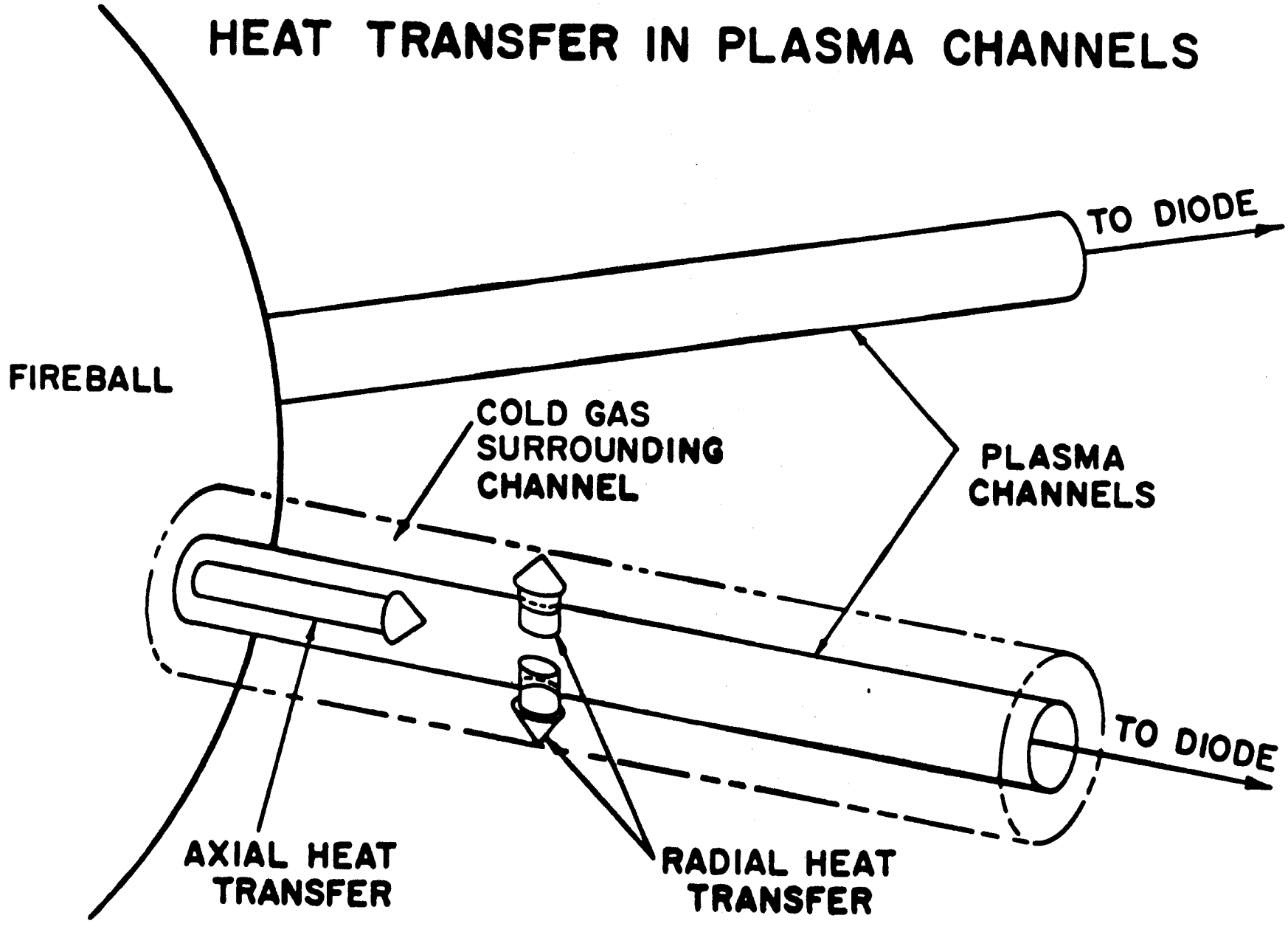

Fig. 3. Schematic Picture of Channels.

improved computer model and will discuss the importance of the radial behavior to the axial microfireball propagation. We will present improved simulations for TDF parameters.

2. Computational Method

Two one-dimensional Lagrangian hydrodynamics computer codes with multi-frequency radiative heat transfer have been used to model the two-dimensional behavior of microfireball propagation in a plasma channel. The radial behavior is modeled with the Z-PINCH computer code.[11] Axial microfireball propagation is simulated with MFFIRE.[12]

The Z-PINCH code has one-dimensional Lagrangian hydrodynamics to model the radial motion of the channel. Electrical current profiles computed by this code are used to calculate the magnetohydrodynamic contribution to the pressure terms that drive the pinching of the channel. The current profiles are dependent upon the temperature profile through a temperature dependent resistivity. The heat transfer from the center of the channel out to cold background gas is determined through the use of equation-of-state tables provided by the MIXERG[13] code and multifrequency radiative heat transfer.

The MFFIRE computer code uses very similar techniques to model the axial behavior of the microfireball in the plasma channels. There are no electrical currents, magnetic fields or magnetohydrodynamic forces in MFFIRE. MFFIRE does, however, compute the deposition in the channels and background gas of x-rays with a prescribed spectrum and ions of a given species and energy that emanated from the center of a sphere, the axis of a cylinder, or the edge of a slab. Except for these differences, MFFIRE and Z-PINCH have identical heat transfer and hydrodynamics.

A four step procedure is used to simulate the two-dimensional behavior with these two one-dimensional codes. First, MFFIRE is used to calculate the temperature profiles in the plasma channels and the background gas due to their initial temperatures and the deposition of the target generated x-rays. The deposition is done in spherical geometry so the x-ray heating sees a $1/R^2$ effect as one moves away from the target microexplosion. The x-ray spectrum in Fig. 4 is taken from the HIBALL[14] study and is the standard spectrum used in several studies. The energy of the target debris ions is included in the lowest energy group of this spectrum. The axial channel and background gas temperatures at the start of hydrodynamic motion are shown in Fig. 5, for the parameters in Table 1 and the x-ray spectrum in Fig. 4. The Z-PINCH code is then used to simulate the radial hydromotion and heat transfer at various points along the channel, using a central channel temperature and a background gas temperature taken from Fig. 5. From the calculations with Z-PINCH a phenomenological radial energy loss function is created as a function of the gas temperature at the center of the channel. Also, the channel radius is determined as a function of time at various points along the channel. MFFIRE is run again with the radial energy loss term included to simulate the axial propagation of the microfireball in the plasma channel.

Results have been obtained for the TDF parameters in Table 1. The results of the radial calculations are presented in the next section and the axial results in the section after that.

3. Results - Radial Behavior

Radial cylindrical magnetohydrodynamic calculations have been performed with the Z-PINCH code at positions near the target, near the diodes, and in

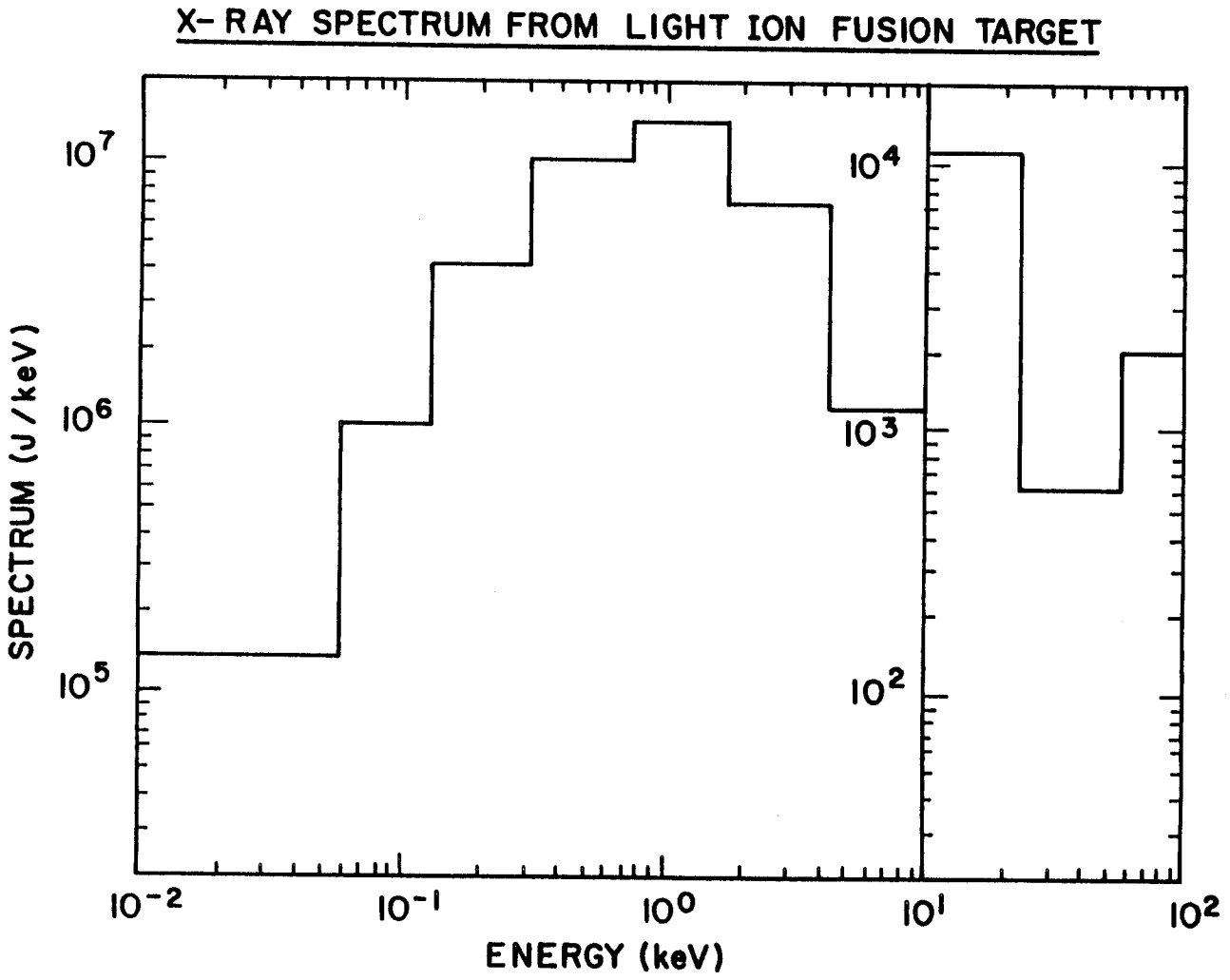

Fig. 4. X-Ray Spectrum Emanating from Target.

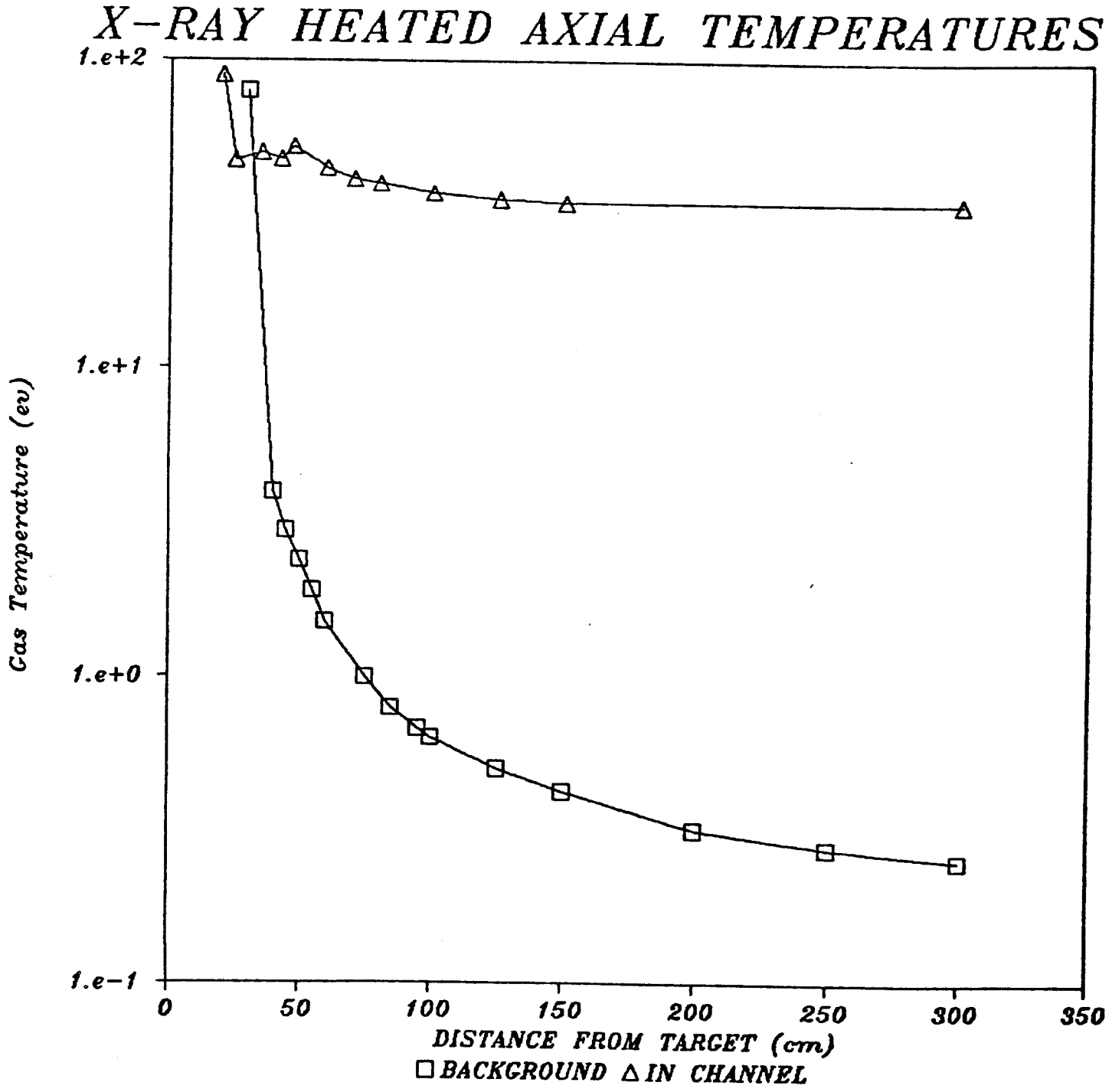

Fig. 5. Temperature Profiles in Background Gas and at Center of Channel After Deposition of Target Generated X-Rays.

between. As seen in Fig. 5, near the target the temperatures in the center of the channels and in the background gas are much higher than in positions farther from the target. We will present results both near the target and at a moderate distance from the target, but will not discuss the situation at the diode because it is not very different from the middle distance case. These results have allowed us to find the radial energy loss as a function of the temperature of the gas at the center of the channels.

The results of simulations at an axial position on the channels 50 cm from the target are depicted in Figs. 6 through 8. These figures show the magnetic field, the gas temperature, and the gas mass density plotted as functions of the distance from the center of the channel. In Fig. 6, one can see the situation at the instant after the x-rays and ions from the target microexplosion deposit their energy in the gas. The central channel gas temperature is 50 eV and the magnetic field reaches a maximum of about 3 kG at a point 1 cm from the center of the channel. The mass density also reached a maximum at a radius of 1 cm and a minimum near the center of the channel of about one tenth of the maximum. Figure 7 shows that by 50 microseconds after the microexplosion the maximum magnetic field has fallen to 5.6×10^{-3} G and the channel radius has spread to about 15 cm. The maximum temperature in the center of the channel is then 0.6 eV and the minimum mass density has risen from 2.4×10^{-6} to 7×10^{-6} g/cm^3. By 110 microseconds after the microexplosion, the case shown in Fig. 8, the magnetic field is negligible and is not shown, the channel radius has grown to more than 20 cm, and the central channel temperature is 0.5 eV. The minimum mass density is 6×10^{-6} g/cm^3.

Calculations at an axial position of the channels 150 cm from the target lead to the results shown in Figs. 9 through 14. The radial hydromotion of

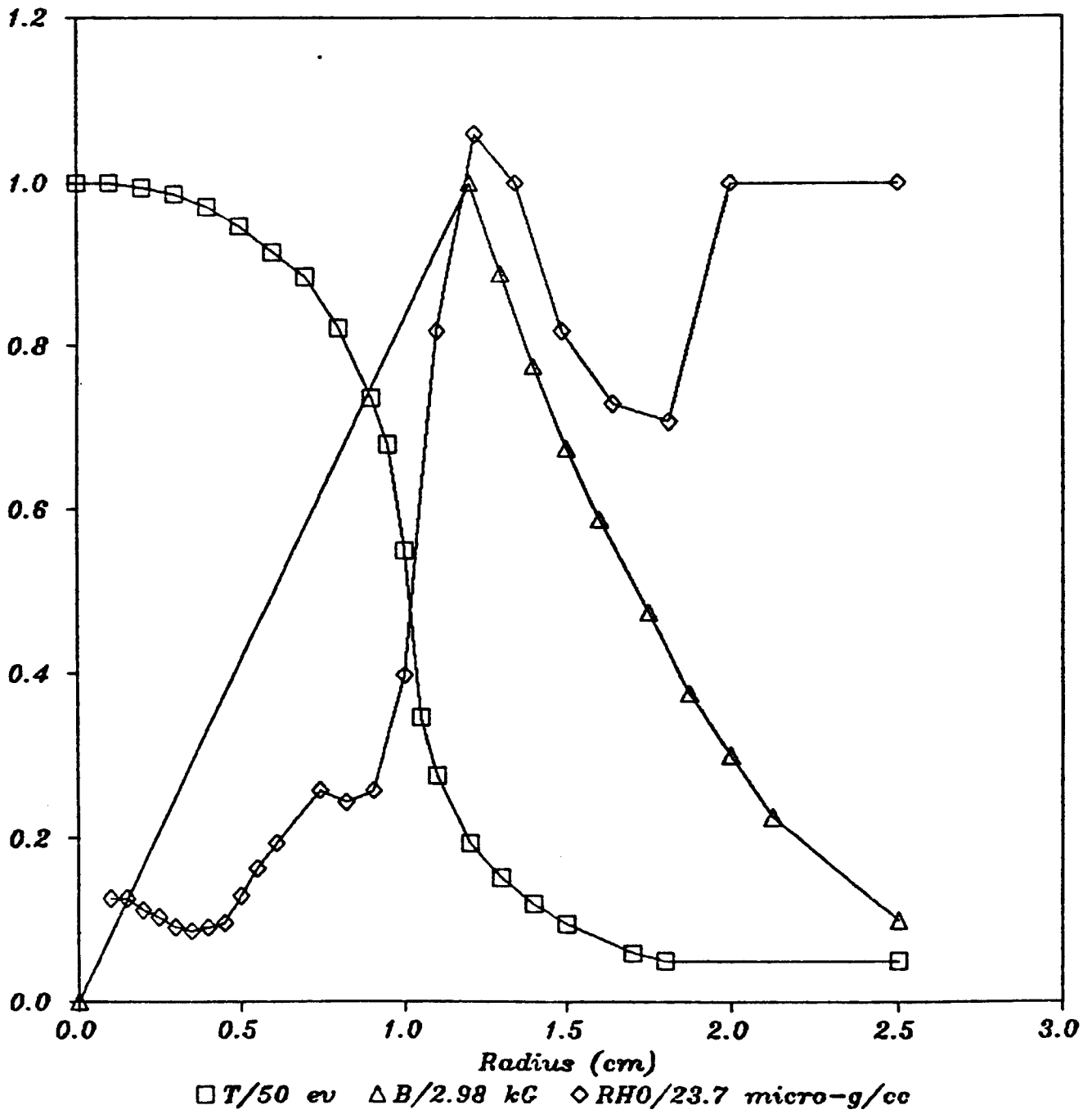

Fig. 6. Magnetic Field, Gas Temperature and Gas Mass Density Versus Distance from the Center of the Channel After the Deposition of Target Generated X-Rays. The Axial Position is 50 cm from the Target.

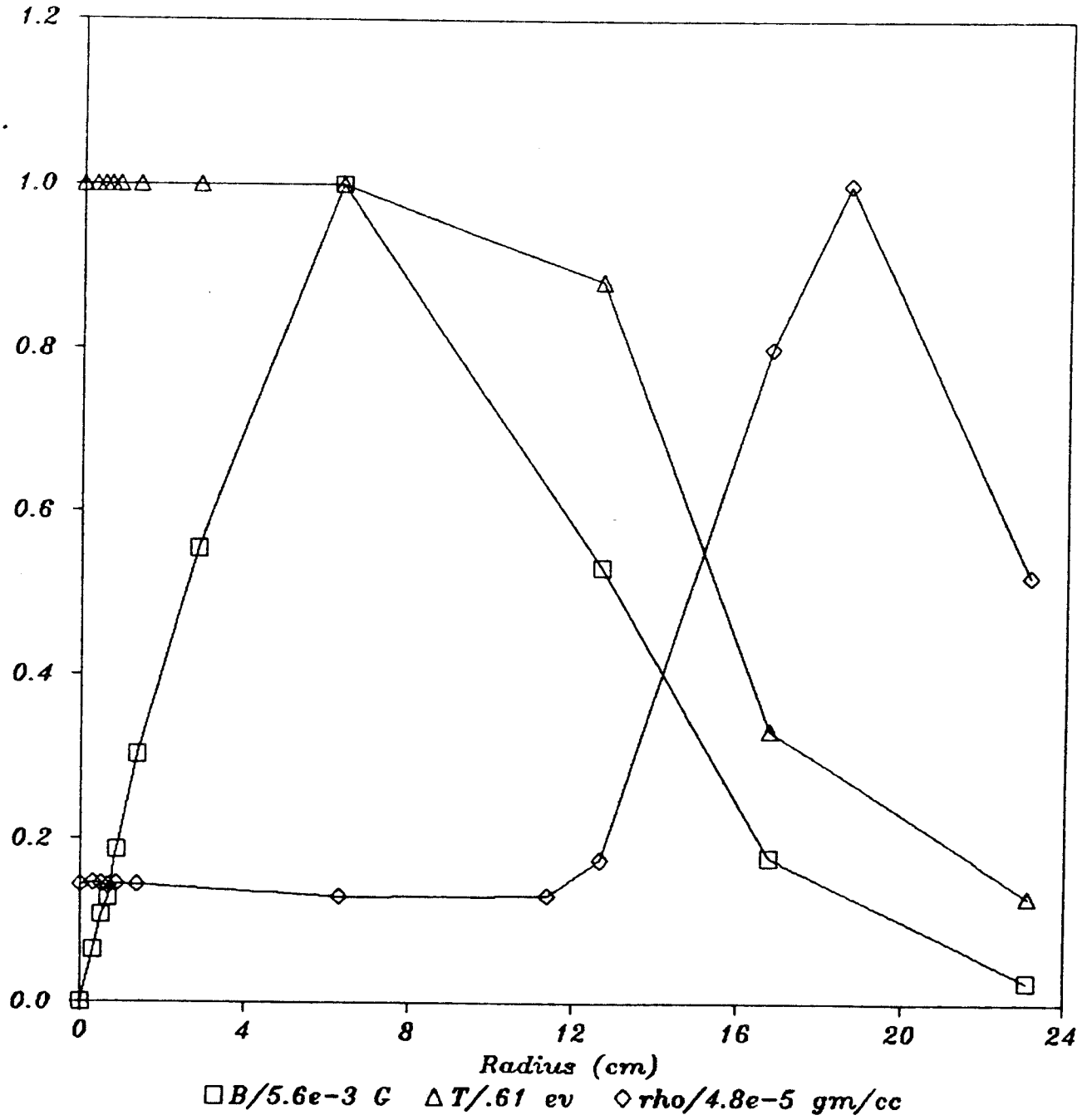

Fig. 7. Magnetic Field, Gas Temperature and Gas Mass Density Versus Distance from the Center of the Channel 50 Microseconds after the Target Microexplosion. The Axial Position is 50 cm from the Target.

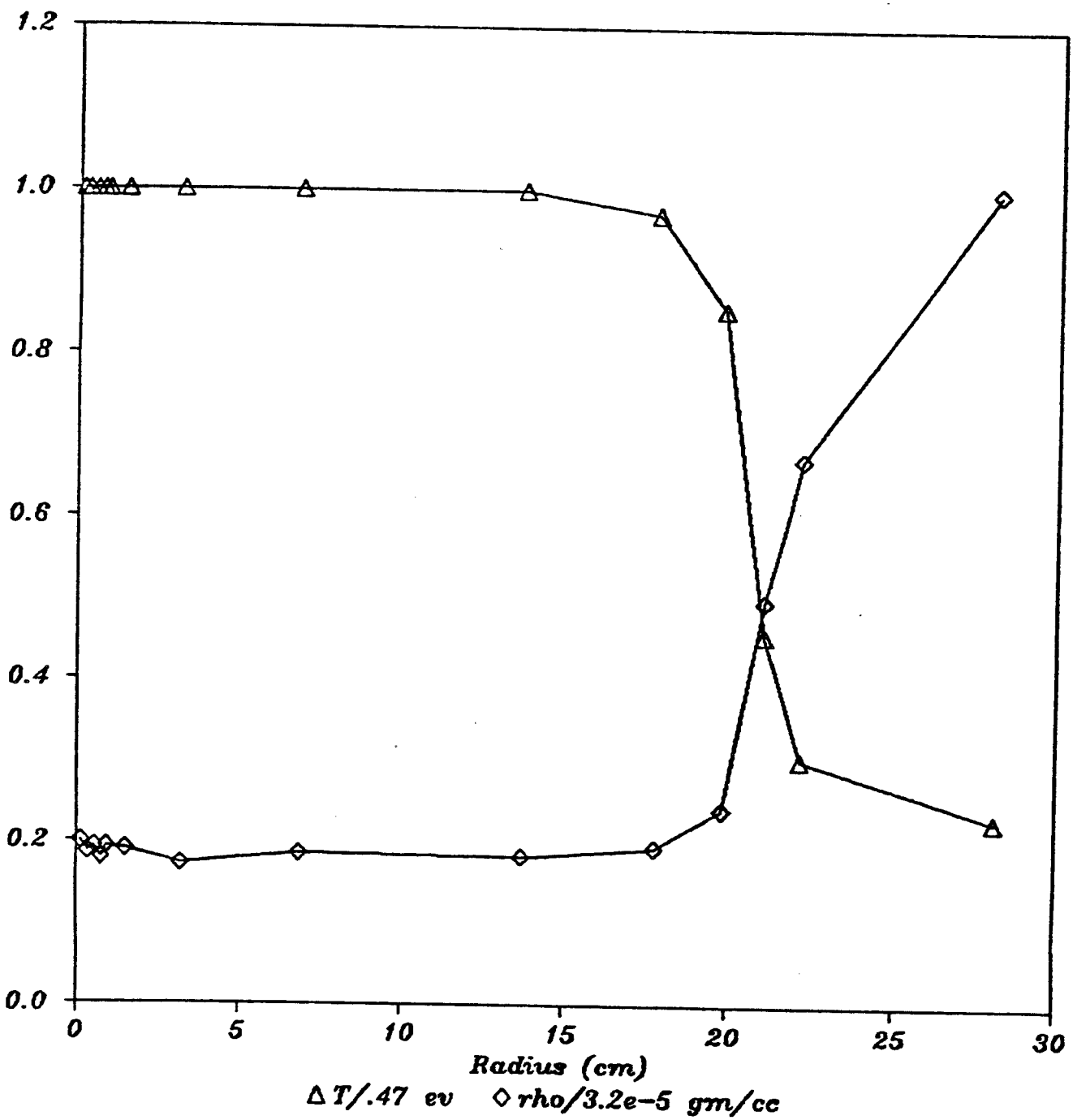

Fig. 8. Gas Temperature and Gas Mass Density Versus Distance from the Center of the Channel 110 Microseconds After the Target Microexplosion. The Axial Position is 50 cm from the Target.

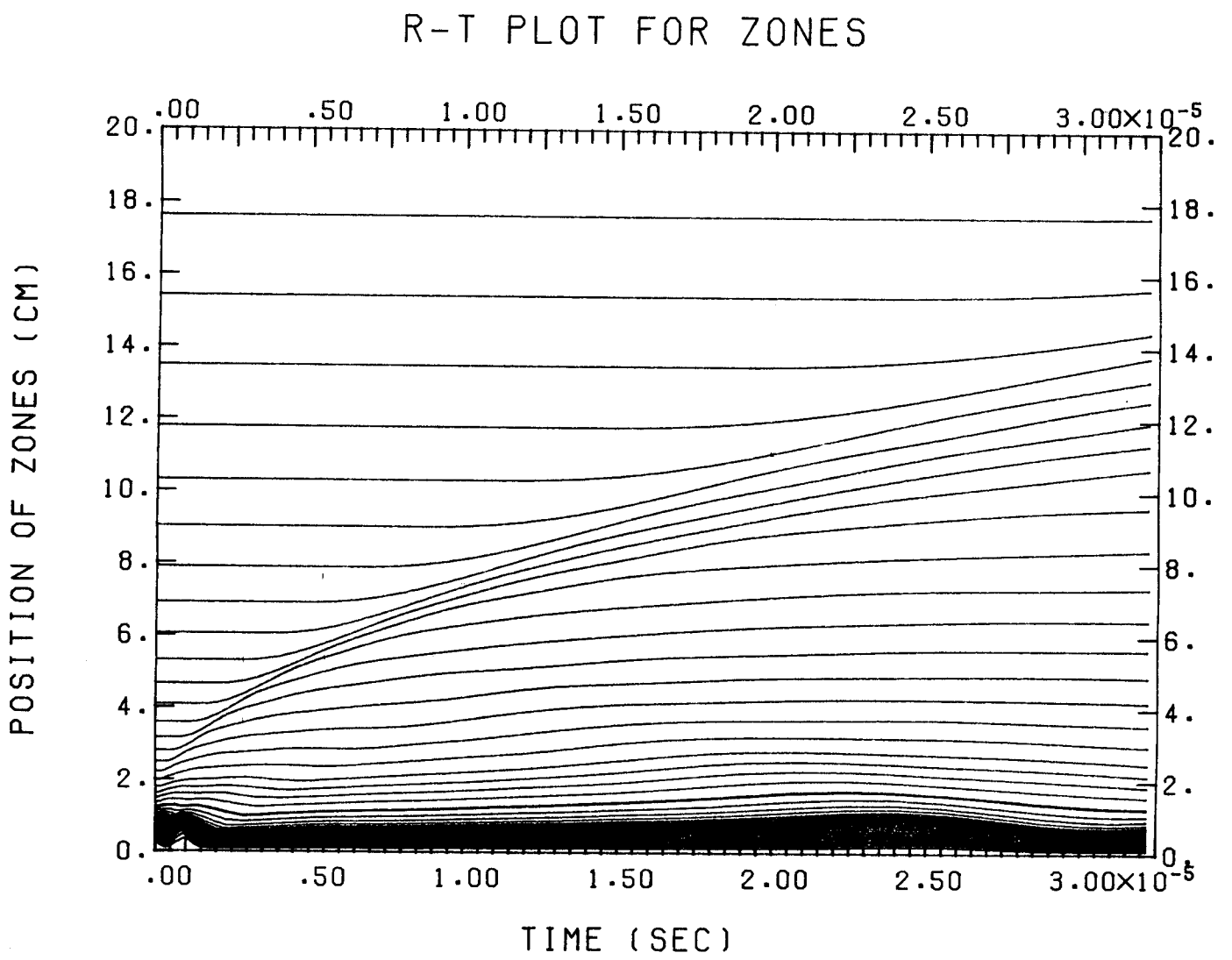

Fig. 9. Radial Hydrodynamic Motion of Channel 150 cm from the Target. The Axial Position is 150 cm from the Target.

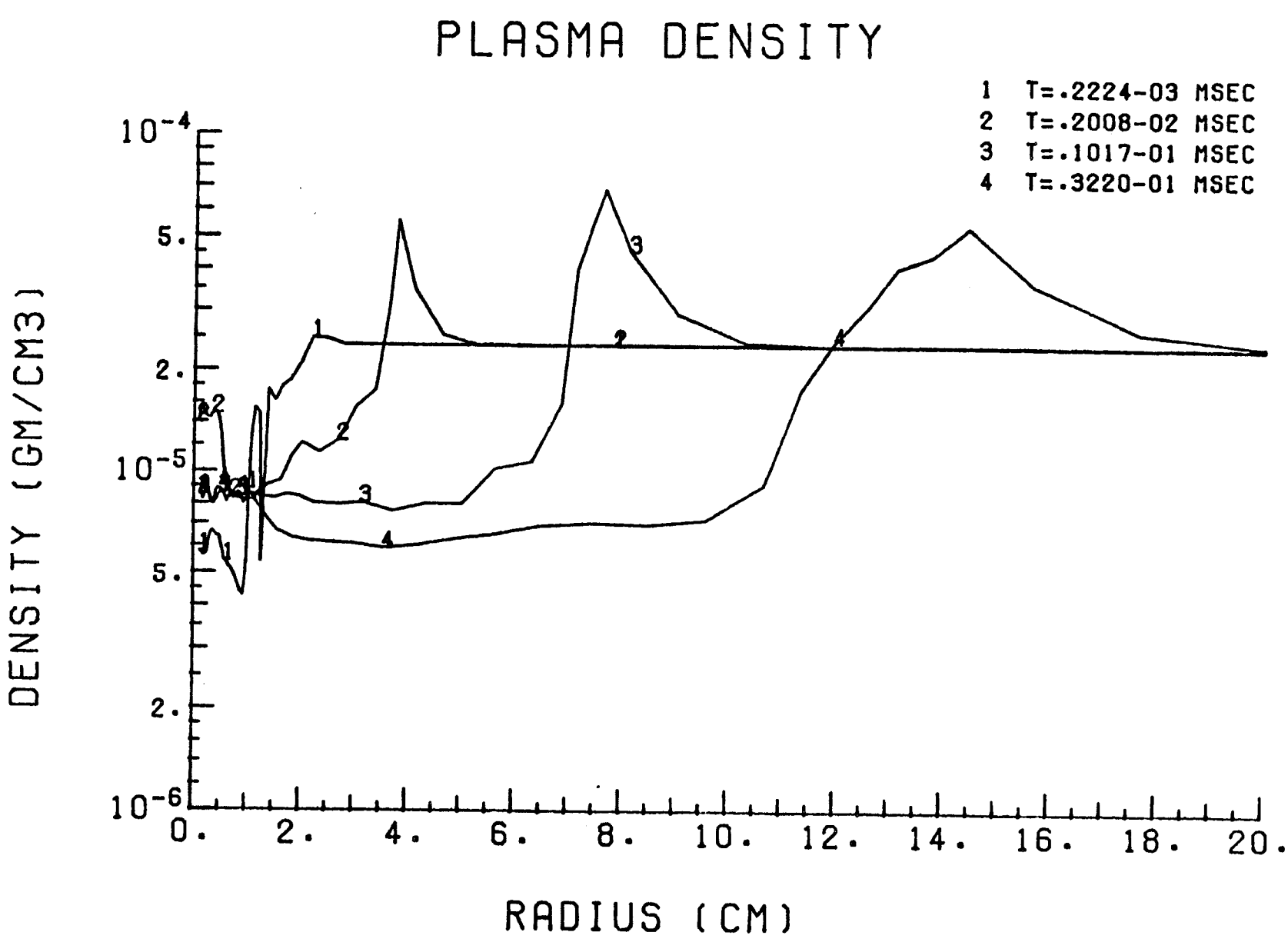

Fig. 10. Gas Density of Channel Versus Distance from Center of Channel at Various Times Shortly After the Target Explosion. The Axial Position is 150 cm from the Target.

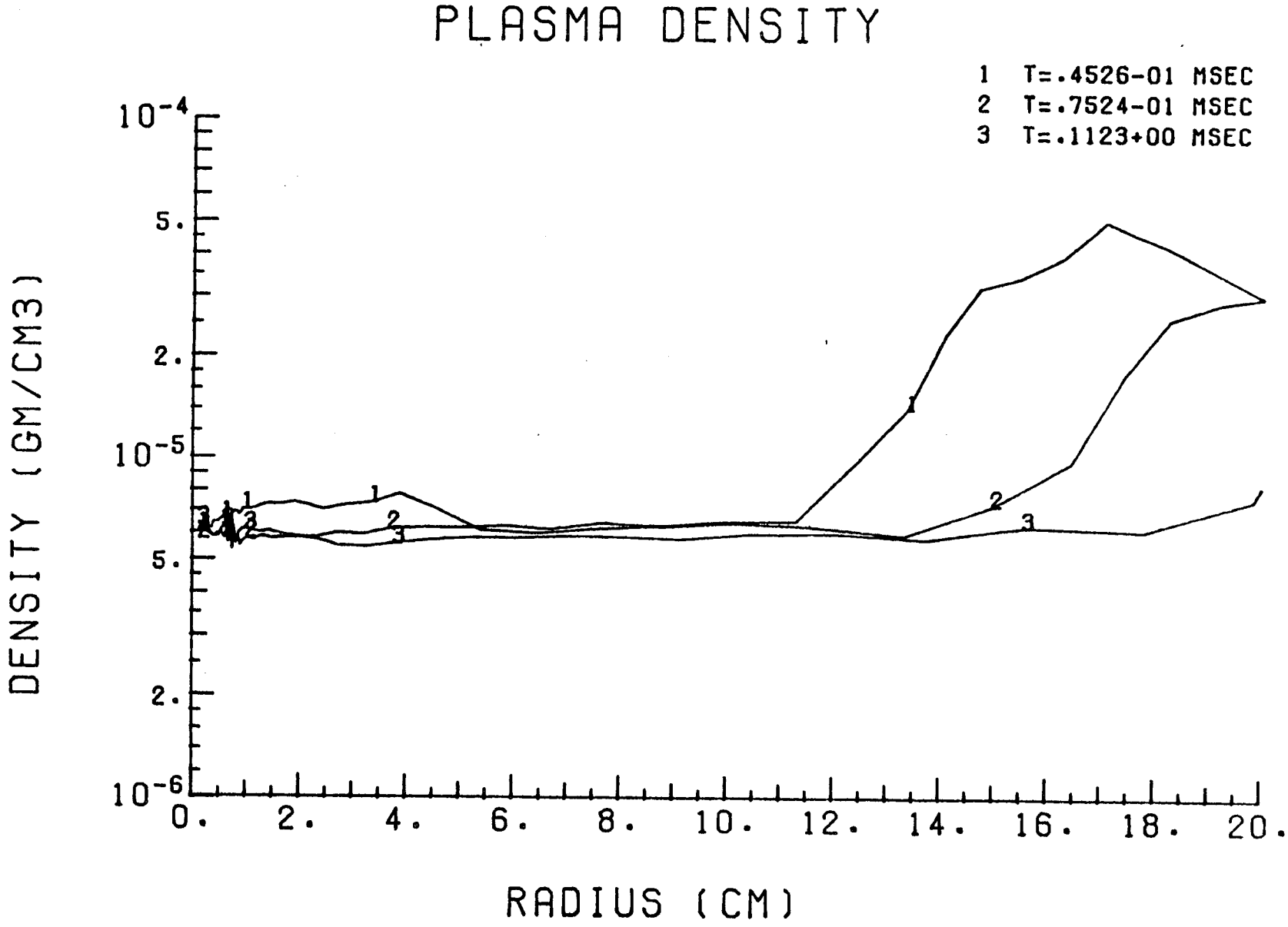

Fig. 11. Gas Density of Channel Versus Distance from Center of Channel at Various Longer Times After the Target Explosion. The Axial Position is 150 cm from the Target.

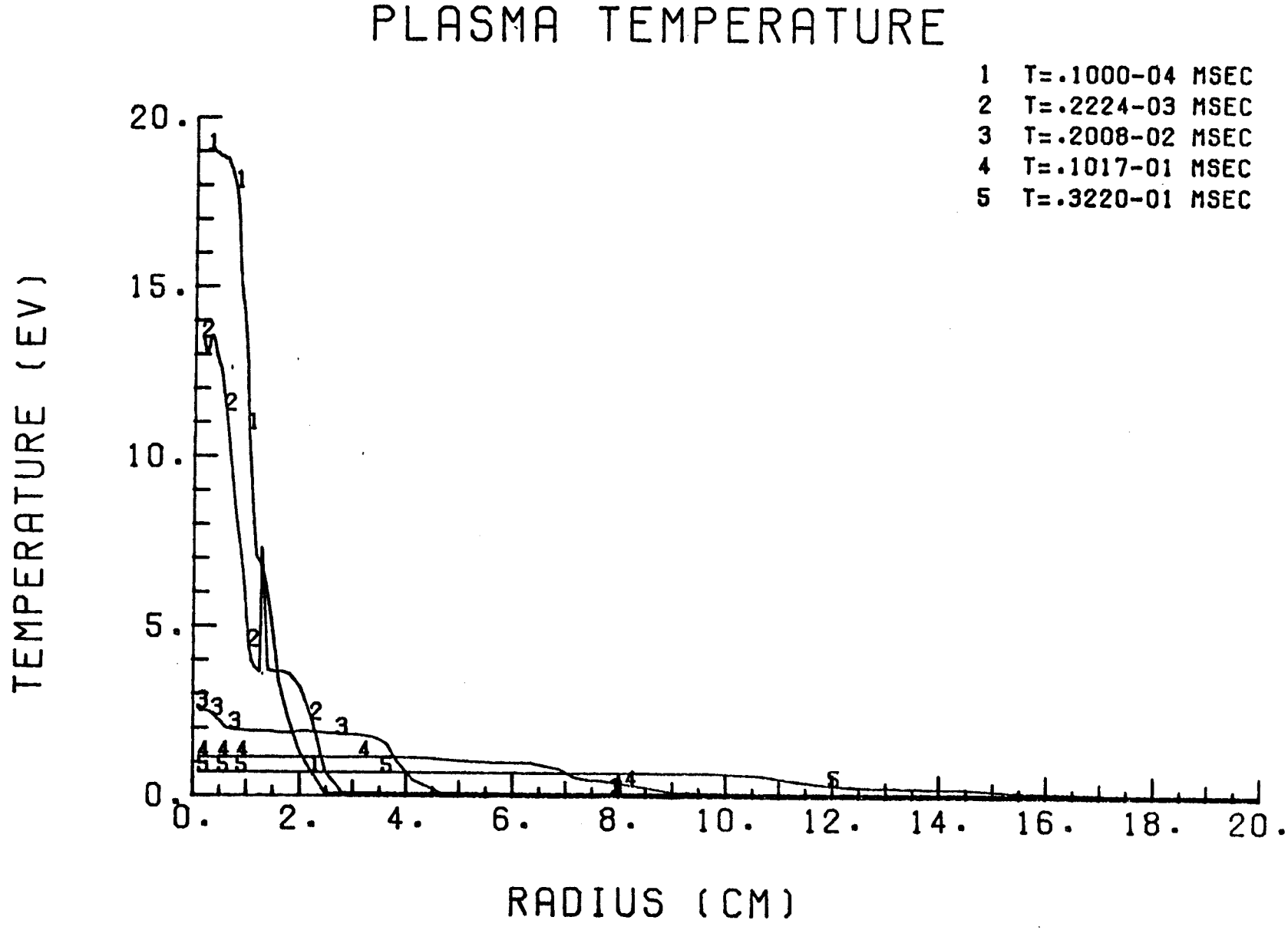

Fig. 12. Gas Temperature Versus Distance from Center of Channel at Various Times Shortly After the Target Explosion. The Axial Position is 150 cm from the Target.

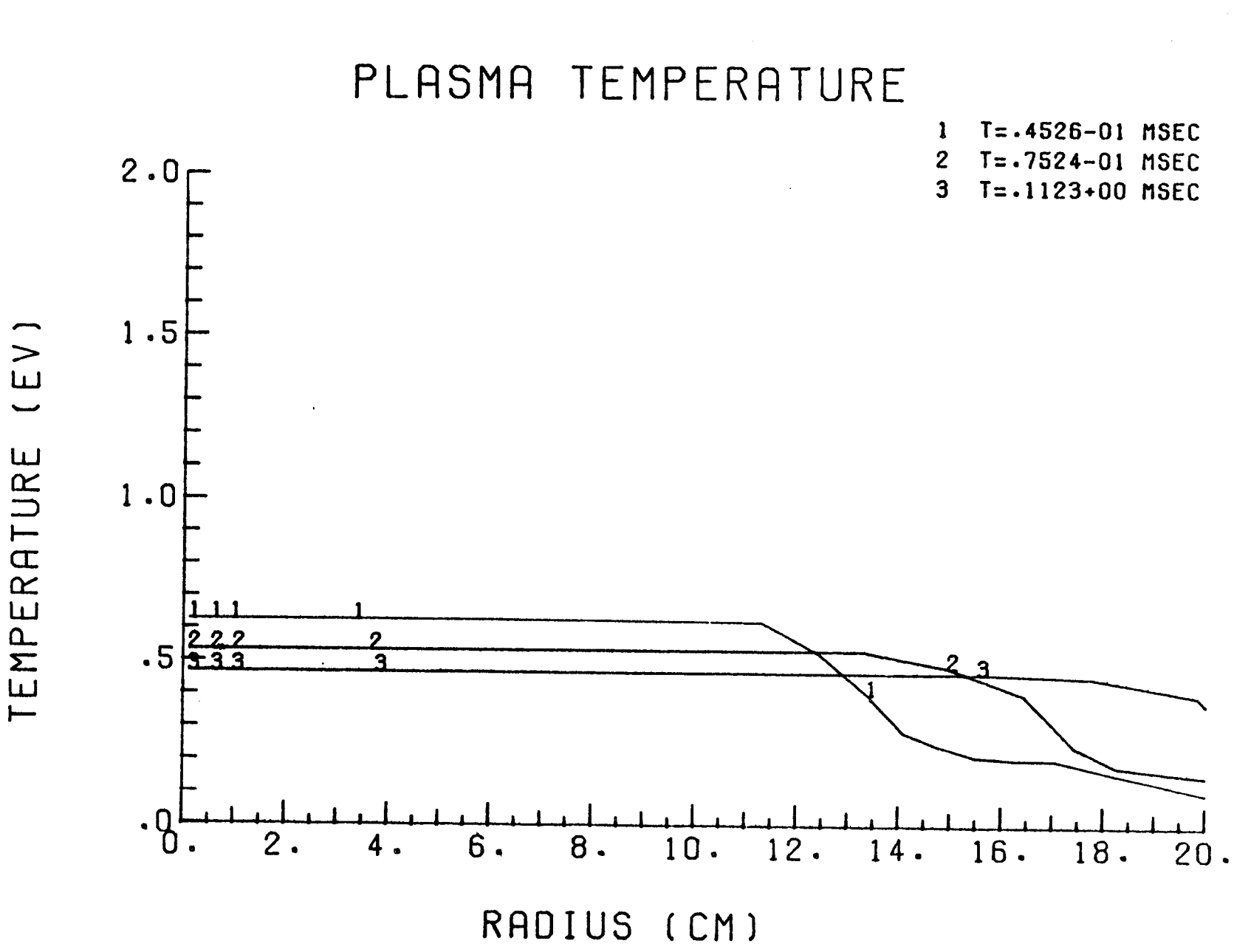

Fig. 13. Gas Temperature Versus Distance from Center of Channel at Various Longer Times After the Target Explosion. The Axial Position is 150 cm from the Target.

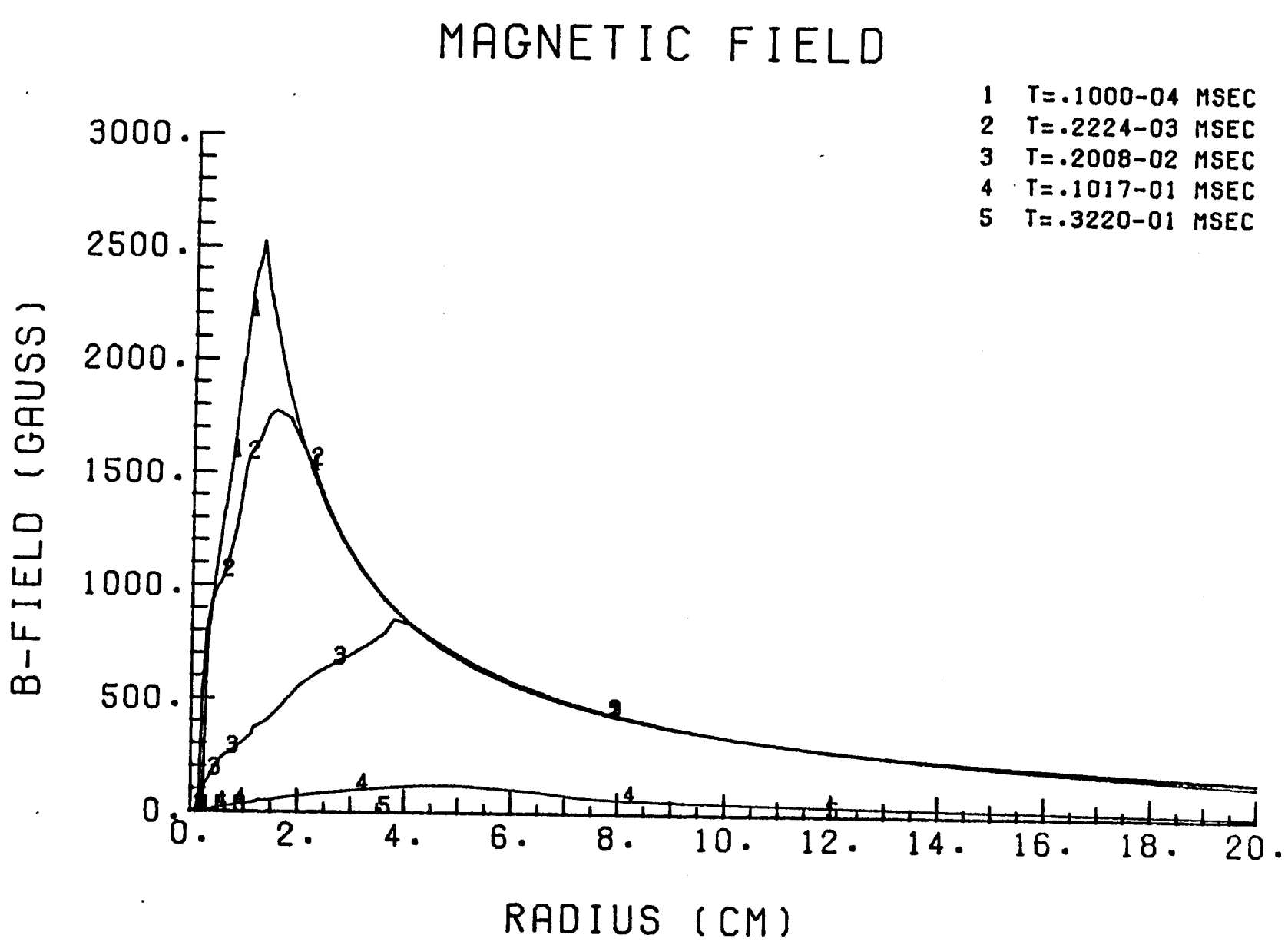

Fig. 14. Azimuthal Magnetic Field Versus Distance from Center of Channel at Various Times After the Target Explosion. The Axial Position is 150 cm from the Target.

the channel, shown in Fig. 9 where the positions of Lagrangian zone boundaries are plotted against time, is mostly outward away from the center of the channel. At 30 microseconds after the microexplosion a cylindrically expanding shock has reached a point 14 cm from the center of the channel. This outward motion also appears when one plots the gas mass density of the channel against radial position for various times as in Figs. 10 and 11. As may be seen in Fig. 10, where the mass density is plotted at relatively early times, at 30 microseconds after the microexplosion most of the channel out to 10 cm from the channel center is at 6×10^{-6} g/cm^3 while there is a maximum density at 15 cm of ten times that value. That ratio of the maximum to minimum mass density is the same at 2 and 10 microseconds after the microexplosion. One can see the mass density at later times in Fig. 11, where it is of interest that at 110 microseconds the channel mass density is 6×10^{-6} g/cm^3 out to a radius of 20 cm. The high gas temperatures in the channel center, shown in Figs. 12 and 13 where the temperature is plotted against radial position at early and later times respectively, cause large pressure gradients that drive this outward directed hydromotion. Radial radiative heat transfer and decompression of the channel center reduce the temperature at the center of the channel from 35 eV after the deposition of the x-rays and ions to 1 eV at 10 microseconds to 0.47 eV at 110 microseconds after the microexplosion. The outward spreading of the hot region in the channel center exactly follows the radial shock that one sees in Figs. 9, 10 and 11. The magnetic field quickly falls and somewhat spreads out as is shown in Fig. 14. The field has effectively vanished by 30 microseconds after the target explosion.

The calculations done at a point 150 cm from the target are more representative of the typical behavior all along the channel than the calculations

near to the target; therefore we have used them to find the radial energy loss as a function of the central channel temperature. In fact, past the very early times the calculations close to the target are almost identical to those at 150 cm from the target. The radial energy loss term is defined as the power lost per unit volume of channel. All parts of the channel with a temperature greater than half of the maximum are defined as part of this volume and the central channel temperature corresponding to this energy loss term is taken as the average over this same volume. Figure 15 shows the radial energy loss term plotted against the central channel temperature. The data points come from calculations of the energy loss term on specific time steps in Z-PINCH runs, while the solid line represents the piecewise linear functional form that best approximates these data. The term varies by five orders of magnitude as the temperature changes by about one order of magnitude. This occurs because the dominant form of energy loss is through thermal radiation.

4. Results - Axial Behavior

As the energy of the microfireball moves axially down the plasma channel, it loses energy radially as prescribed by the radial energy loss term shown in Fig. 15. A version of MFFIRE modified to include this energy loss simulates the axial behavior of the microfireball. Since the channel radius is assumed to be independent of the axial position along the channel, it is appropriate to run MFFIRE in its slab mode.

Results of MFFIRE simulations have shown that there is very little hydromotion because the energy that could drive it is very quickly radiated away, both axially and radially. One can study the axial heat transfer by examining the axial temperature profiles plotted at different times, shown in Fig. 16.

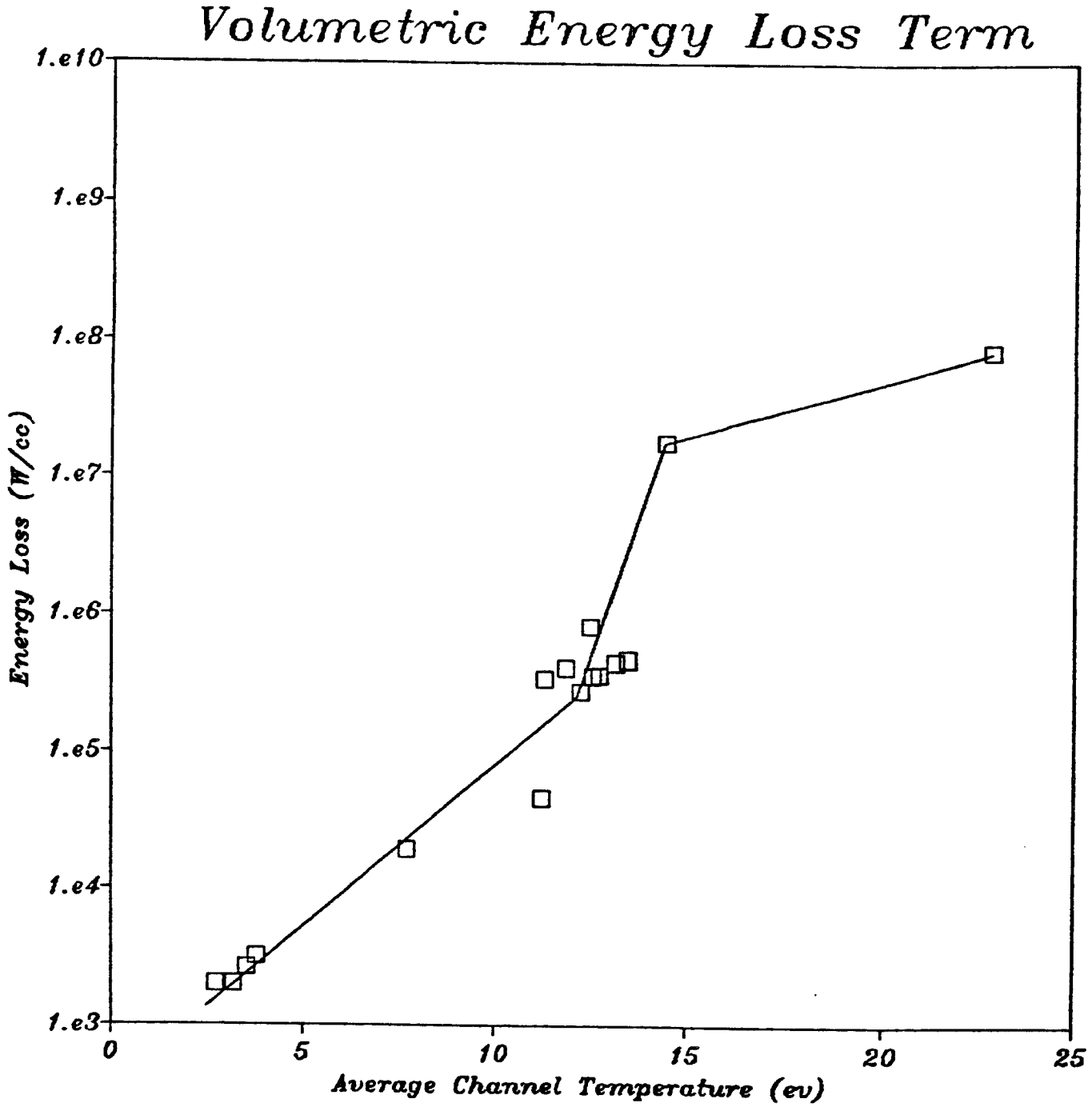

Fig. 15. Radial Energy Loss Coefficient Versus Gas Temperature in the Center of the Channel.

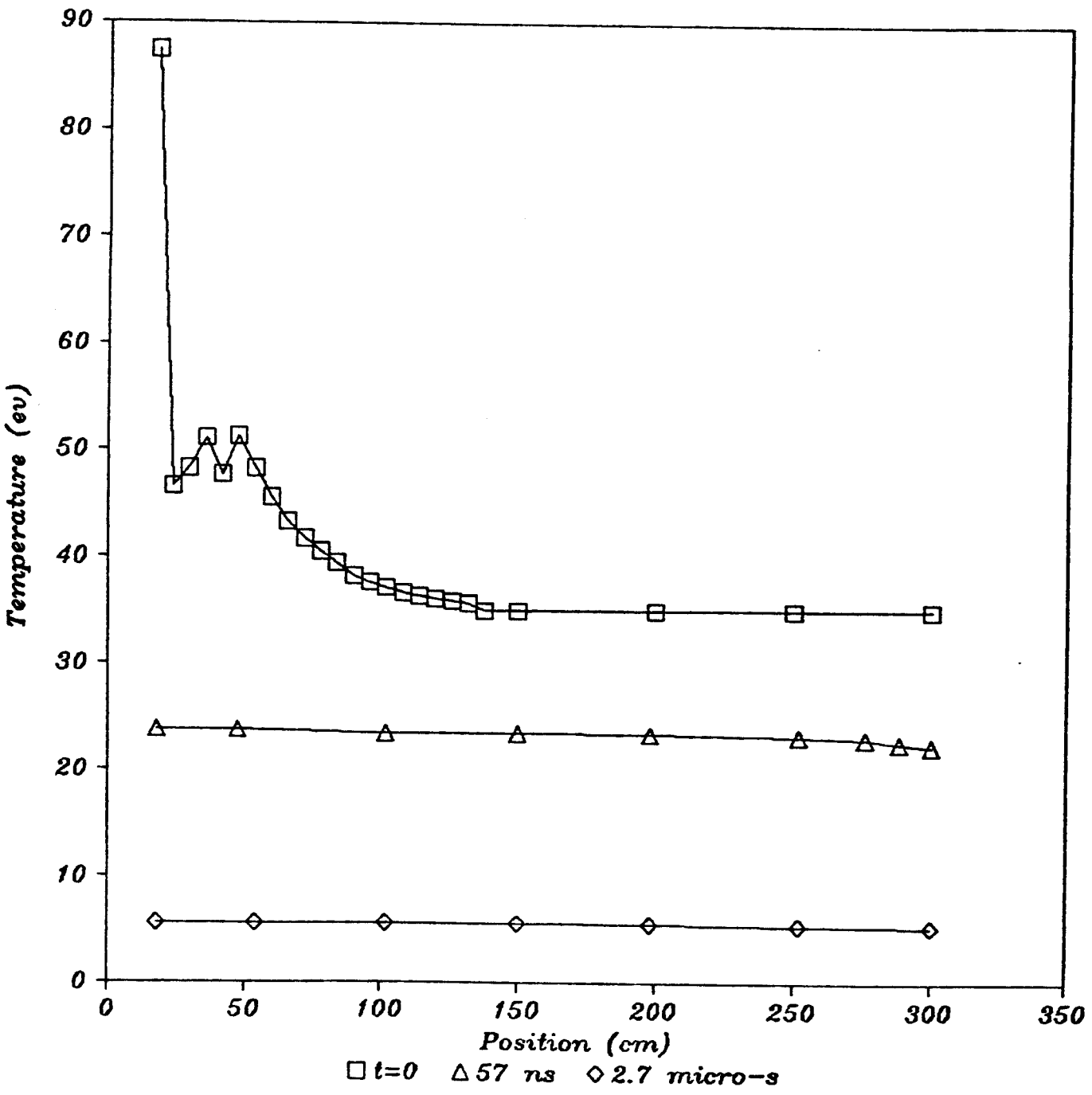

Fig. 16. Gas Temperatures Versus Axial Position Along the Channel at Various Times After the Target Microexplosion.

The axial temperature profile falls from the initial curve, that has a maximum near the target of 87 eV and a minimum of 35 eV, to flat profiles of 23 eV at 57 nanoseconds and 6 eV at 2.7 microseconds. Very close to half of the energy lost out of each channel exits radially and half axially. Each channel contains 10.03 kJ of energy after the deposition of target x-rays and ions, 4.85 kJ in radiation and the rest in the gas. 4.75 kJ are radiated out to the diode end of the channel over the first 670 microseconds and 4.73 kJ are radiated axially, with 0.55 kJ remaining in the channel.

5. Discussion and Conclusions

We have simulated the propagation of energy from a microexplosion of a fusion target through z-pinch plasma channels for the case of the TDF. We have used two one-dimensional computer codes to model two-dimensional phenomena. We feel that computational results from using the method outlined in Section 2 give us a basis for understanding the important physics of the problem.

One finds from our computational results that radiative heat transfer, both radial and axial, is very important, and that axial hydromotion is not important. Roughly half of the initial energy is radiated radially and half axially, with only a small fraction remaining in the gas. A considerable part of the initial energy in each channel is due to the passage of the ion beam through the channel and the formation of the channel.

Though axial hydromotion is not significant, radial expansion of the channel could be important. We have previously calculated that a spherical shock wave in the cold background gas arrives at the first wall 350 microseconds after the microexplosion.[15] One can extrapolate our radial results

out to that time and find that the channel radius is about 50 cm when the spherical shock reaches the wall. If the TDF has 8 channels, 800 cm of the 1885 cm of the circumference in the plane of the diodes are covered by channels. The interaction of the spherical microfireball with the expanded channels is not understood, but it clearly must be considered.

Acknowledgement

This work was supported by the U.S. Department of Energy under contract #DE-AS08-83DP40184.

References

1. P.A. Miller, R.I. Butler, M. Cowan, J.R. Freeman, J.W. Poukey, T.P. Wright, and G. Yonas, "Propagation of Pinched Electron Beams for Pellet Fusion," Phys. Rev. Lett. 39, 92 (1977).

2. G. Yonas, "Fusion Power with Particle Beams," Sci. Amer. 239, 50 (1978).

3. J.R. Freeman, L. Baker and D.L. Cook, "Plasma Channels for Intense-Light-Ion-Beam Reactors," Nucl. Fusion 22, 383 (1982).

4. D.W. Koopman and K.A. Saum, "Formation and Guiding of High-Velocity Electrical Streamers by Laser-Induced Ionization," J. App. Phys. 44, 5328 (1973).

5. J.R. Greig, D.W. Koopman, R.F. Fernsler, R.E. Pechecek, I.M. Vitkovitsky and A.W. Ali, "Electrical Discharges Guided by Pulsed CO_2-Laser Radiation," Phys. Rev. Lett. 41, 174 (1978).

6. D.W. Koopman, J.R. Greig, R.E. Pechecek, A.W. Ali, I.M. Vitkovitsky and R.F. Fernsler, "CO_2-Laser Produced Channels for Guiding Long Sparks in Air," J. DePhysique (2077, Suppl. 7) 40, 419 (1979).

7. J.R. Greig, "Reduced-Density Channels in Gases at Atmospheric Pressure," Bull. Amer. Phys. Soc. 25, 942 (1980).

8. M. Raleigh, J.R. Greig, R.E. Pechecek and E. Laikin, "Laser-Initiated, Reduced Density Channels for Transporting Charged Particle Beams," NRL Memorandum Report 4380, U.S. Naval Research Laboratory (February 1981).

9. G.A. Moses et al., "Light Ion Fusion Target Development Facility Preconceptual Design," Nucl. Tech./Fusion 4, 961 (September 1983).

10. R.R. Peterson, K.J. Lee and G.A. Moses, "Fireball Dynamics in Preformed Plasma Channels of Light Ion Beam Fusion Reactors," Bull. Amer. Phys. Soc. 26, 900 (October 1981).

11. J.J. Watrous, G.A. Moses and R.R. Peterson, "Z-PINCH - A Multifrequency Radiative Transfer Magnetohydrodynamics Computer Code," University of Wisconsin Fusion Technology Institute Report UWFDM-584 (June 1984).

12. G.A. Moses, T.J. McCarville and R.R. Peterson, "Documentation for MFFIRE, A Multifrequency Radiative Transfer Version of FIRE," University of Wisconsin Fusion Technology Institute Report UWFDM-458 (March 1982, Revised August 1984).

13. R.R. Peterson and G.A. Moses, "MIXERG - An Equation of State and Opacity Computer Code," Computer Physics Communications 28, 405 (1983).

14. B. Badger et al., "HIBALL - A Conceptual Heavy Ion Beam Driven Fusion Reactor Study," University of Wisconsin Fusion Technology Institute Report UWFDM-450 (December 1981).

15. R.R. Peterson and G.A. Moses, "Target Explosion Generated Fireballs in the Nitrogen Filled Target Chamber of the Light Ion Fusion Target Development Facility," Nucl. Tech./Fusion 4, 860 (September 1983).